Moiré patterns and step edges on few-layer graphene grown on nickel films*

Ke Fen(柯 芬)[a], Yin Xiu-Li(尹秀丽)[a], Tong Nai(佟 鼐)[a],
Lin Chen-Fang(林陈昉)[a], Liu Nan(刘 楠)[b], Zhao Ru-Guang(赵汝光)[a],
Fu Lei(付 磊)[b], Liu Zhong-Fan(刘忠范)[b], and Hu Zong-Hai(胡宗海)[a)c)†]

[a] *State Key Laboratory for Artificial Microstructures and Mesoscopic Physics, School of Physics, Peking University, Beijing* 100871, *China*
[b] *Center for Nanochemistry (CNC), Beijing National Laboratory for Molecular Sciences, State Key Laboratory for Structural Chemistry of Unstable and Stable Species, College of Chemistry and Molecular Engineering, Academy for Advanced Interdisciplinary Studies, Peking University, Beijing* 100871, *China*
[c] *Collaborative Innovation Center for Quantum Matter, Beijing* 100871, *China*

(Received 21 April 2014; revised manuscript received 14 May 2014; published online 24 September 2014)

Few-layer graphene grown on Ni thin films has been studied by scanning tunneling microscopy. In most areas on the surfaces, moiré patterns resulted from rotational stacking faults were observed. At a bias lower than 200 mV, only one sublattice shows up in regions without moiré patterns while both sublattices are seen in regions with moiré pattens. This phenomenon can be used to identify AB stacked regions. The scattering characteristics at various types of step edges are different from those of monolayer graphene edges, either armchair or zigzag.

Keywords: scanning tunneling microscopy, few-layer graphene, stacking order, step edge

PACS: 68.37.Ef, 68.65.Cd, 73.21.Cd,73.22.Pr **DOI:** 10.1088/1674-1056/23/11/116801

1. Introduction

Graphene has attracted tremendous interest in recent years due to its remarkable properties and great potential for various applications. While the graphene monolayer has been studied most extensively, bilayer and few-layer graphenes (FLG) have received increasing attention.[1–9] The properties of FLG are strongly influenced not only by the number of layers but also the stacking order.[3–7] Bernal (AB) stacking results in parabolic dispersion near the charge neutrality point. Rotational stacking mostly leads to characteristics similar to those of monolayer graphene, although the Fermi velocity is renormalized and points of van Hove singularity develop depending on the rotational angle.[3,10] Therefore, accurate measurement of the angle (including zero value) is an important issue.

Among many transition metal substrates, nickel can readily produce FLG. It is widely exploited with different methods (CVD method and surface segregation technique), on various nickel substrates (film,[7,11–14] foil[15,16] and single crystal,[17]) and in different environments, from ambient pressure[7,11] to ultrahigh vacuum.[17] The size of single-crystal graphene pieces produced by these methods is usually microns or smaller in dimension.

The boundaries of these graphene pieces appear as step edges on FLG. Valuable information about the number of layers and stacking order can be drawn from the atomic structures around these step edges.[3,18] Moreover, edges play a key role in the electronic structure of graphene nanoribbons.[19–22] Scattering and quantum interference at the edges significantly affect the transport properties of graphene.[23,24] There are two fundamental types of graphene edges: armchair and zigzag. Scanning tunneling microscopy (STM) has been a powerful technique to probe the edge effects. The edge state is only present around zigzag edges.[20] Meanwhile, the scattering behavior is more profound at armchair edges.[25,26] Besides the $(\sqrt{3}\times\sqrt{3})R30^\circ$ scattering pattern observed around both types of edges, a honeycomb pattern has only been reported around armchair edges.[25,26] However, most of these studies were conducted on monolayer graphene. Because of the interlayer coupling, the edge effects in FLG can be more complicated. This is one subject of the current work.

On the other hand, rotational stacking induced moiré patterns have been the subject of intensive experimental and theoretical research.[3,27] They are widely used to deduce the twist angle between two adjacent layers[18,28]

$$D = d/[2\sin(\theta/2)], \tag{1}$$

where D is the period of the moiré pattern and $d = 0.246$ nm is the lattice constant of graphene. This formula is based on the hypothesis that only the geometrical alignment between the top two layers determines the moiré pattern, other factors (such as contributions from other layers) can be neglected.

*Project supported by the National Basic Research Program of China (Grant No. 2012CB921300), the National Natural Science Foundation of China (Grant Nos. 11074005 and 91021007), and the Chinese Ministry of Education.

†Corresponding author. E-mail: zhhu@pku.edu.cn

© 2014 Chinese Physical Society and IOP Publishing Ltd

More study is needed for a complete and accurate understanding of moiré structures on FLG.

There is another long term issue related to stacking. Graphene has a honeycomb structure. Yet in AB stacked regions on graphite, only one triangular sublattice consisted of half of the carbon atoms is visible in STM measurements.[29] This can be explained by that the sublattice right atop the carbon atoms of the second layer has a much lower local density of states than the other, resulting in dark carbon sites in STM images.[30] However, occasionally both sublattices are simultaneously seen on graphite in STM, even at low bias, which is apparently contradictory to the above theory.[31,32] This puzzle has not been clearly resolved for a long time.

In this work, we investigate the atomic structures of the step edges and moiré patterns on FLG on Ni films. Rotational stacking dominates on FLG grown by segregation. At a bias lower than 200 mV, only one sublattice shows up in STM in regions without moiré while both sublattices are seen in regions with moiré, clarifying the long term puzzle. The scattering characteristics at various types of step edges are different from those at armchair or zigzag monolayer graphene edges. We expect this paper to provide a better understanding for various features on FLG.

2. Experimental

The graphene samples were grown using the method reported previously.[33] Briefly, polycrystalline Ni films (about 200-nm thick) were prepared by evaporating Ni (> 99.9 wt% Ni, 0.008 wt% C) onto SiO_2/Si substrates with an ultrahigh vacuum (UHV) electron beam deposition method (ULS400, Balzers). The evaporation rate was about 0.15 nm/s with the substrate kept at room temperature. The growth of graphene was conducted by annealing the Ni films at 900 °C–1100 °C for 3–10 min at 0.4×10^{-3}–4×10^{-3} Pa and then cooling down to room temperature inside a vacuum annealing furnace (VTHK-350, Beijing Technol Science Co., Ltd.). Usually, graphene samples of 10 mm×10 mm in size were prepared and cut into four pieces for STM, LEED and Raman experiments.

The samples were degassed at about 150 °C in UHV with a base pressure below 1×10^{-9} mbar for about 2 h before STM and LEED measurements. STM was performed in constant-current mode with mechanically polished Pt/Ir tips, and all given voltages were referred to a sample. The LEED beam size was about 0.2 mm in diameter.

3. Results and discussion

Figure 1(a) shows representative Raman spectra measured (with a 514-nm excitation wavelength) on the samples. Due to the stacking disorder in the first few layers of our samples, which will be shown later, it is difficult to determine the exact thickness from the Raman spectrum.[7,11,33]

Figure 1(b) shows a typical LEED pattern. The spots of the diffraction pattern appear weak and fuzzy on a dim background, indicating that there are many azimuthal orientations of the graphene domains in the sample.

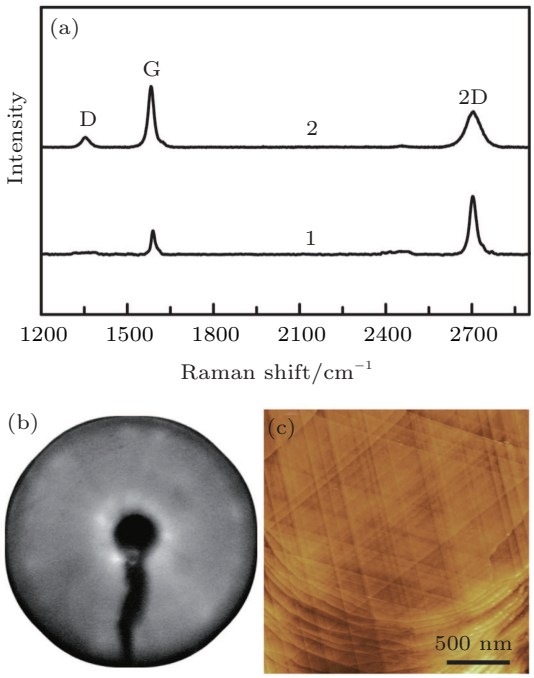


Fig. 1. (color online) (a) Raman spectra taken at different locations on the as-grown graphene film. The D, G, and 2D Raman bands of graphene are labeled, showing a high crystallinity. The spectra were measured with a 514-nm excitation laser and a 50× objective lens. (b) LEED result of the sample. The incident electron beam energy was 61 eV. The dim circle with fuzzy spots reflects many azimuthal angles of graphene domains. (c) A large-scale STM image showing steps of the Ni substrate (scanning conditions: −700 mV, 0.2 nA).

Thermal annealing generates a Ni film microstructure with single-crystalline grains of sizes of several micrometers,[11,13,34] exposing flat (111) facets,[12,13] as shown in Fig. 1(c). The surfaces of these grains have atomically flat and clean terraces, similar to the surface of the single crystal substrates that are used for epitaxial UHV graphene growth. Triangular terraces exist on the grains, as shown in Fig. 2(a). They can extend over tens of nanometers. The monoatomic step height is 0.2 nm. Graphene layers are continuously grown on these terraces. Usually, several layers of graphene were observed on the flat triangular terraces with some small graphene fragments on top. These graphene layers can be easily distinguished by their irregular edges.

The regions covered with and without graphene layers have different corrugations. The line profile in Fig. 2(b) around the graphene edge shows that the lower part with a corrugation of about 0.1 nm is much rougher than the graphene layer. The atomic structure of graphene was never observed in the rough part. Therefore, it can be attributed to an oxidized nickel surface.

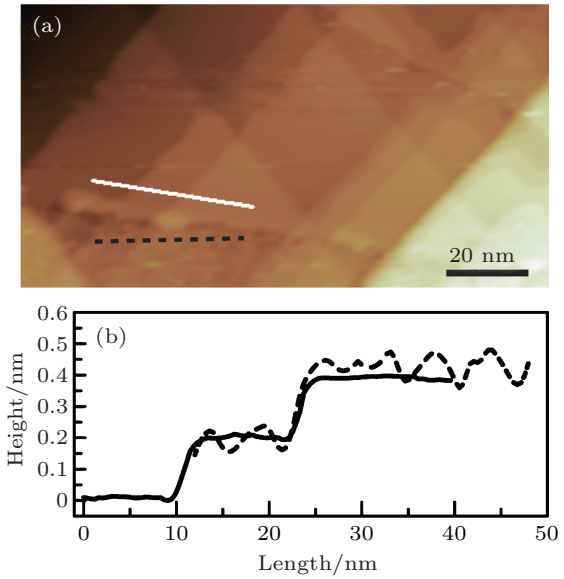


Fig. 2. (color online) (a) A large area STM image (scanning conditions: −500 mV, 0.8 nA). (b) Line profiles along the lines in panel (a), showing a corrugation of 0.01 nm for the graphene covered region and 0.1 nm for the bottom part not covered by graphene.

STM measurements on these samples revealed a common feature; that is, the presence of moiré patterns resulted from twists between graphene layers. In fact, they dominate in the samples. As a comparison, the chances to see moiré patterns on HOPG samples are small because the stacking order is mostly Bernal. Therefore FLG grown on Ni films provides a good system to study the rotational stacking and its influences on graphene properties. In our samples, layers lying above are mostly smaller in size. Therefore, the relation between the moiré pattern and the twist angle can be directly probed at the step edges.

Figure 3 shows one typical edge. The edge of the top layer is marked by a black dashed line in Fig. 3(a). The top layer is smaller in size than the bottom layer. There is a moiré pattern with a period of 3.2 nm on the bottom layer, indicating a twist to the layer beneath. No moiré pattern was observed on the top layer. The zoom-in scanning result in the boxed area is shown in Fig. 3(b). Both layers are atomically resolved, clearly showing the two layers with the same orientation. This explains why no moiré pattern forms on the top layer. The inset of Fig. 3(b) is the corresponding fast-Fourier transform (FFT) result. The regular hexagonal pattern marked by the white circles corresponds to the atomically resolved carbon lattice. The smaller irregular hexagonal pattern corresponds to the scattering pattern caused by the step edge. The edge direction (marked by the solid black line) deviates 5° from the armchair direction (marked by the solid white line) of the graphene lattice. The scattering pattern in the FFT appears as a $(\sqrt{3}\times\sqrt{3})R25°$ pattern, 5° different from the $(\sqrt{3}\times\sqrt{3})R30°$ pattern predicted for monolayer armchair edges.[25,26,35,36] It is also noteworthy that only one sublattice of graphene on the top layer is apparent in STM, indicating AB stacking between layers.[30] Therefore, the edge cannot be simply modeled as a monolayer edge. It is an edge of the top layer of a Bernal bilayer. The differences from monolayer edge scattering are understandable.

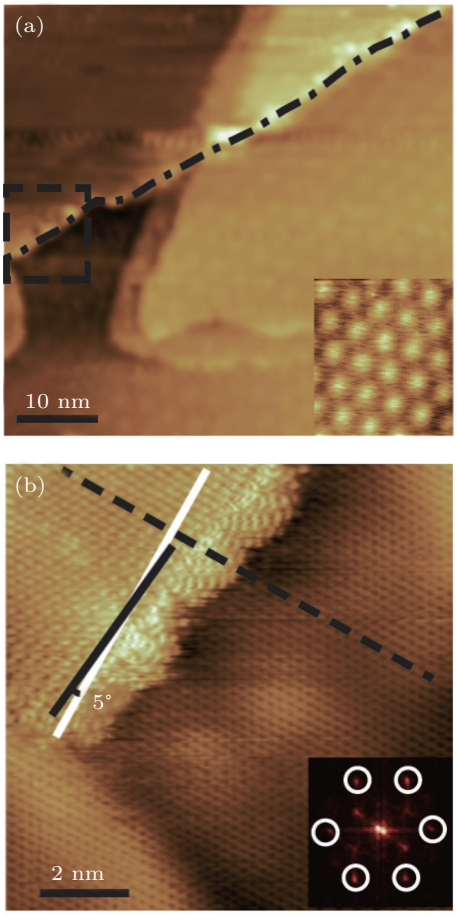


Fig. 3. (color online) STM results at one graphene step edge. (a) There are (not) moiré patterns in the bottom (top) layer. Inset: Moiré pattern of the bottom layer with a period of 3.2 nm. (b) Atomically resolved image in the boxed area in panel (a), showing a scattering pattern. The white solid line and black solid line mark the armchair direction and the step edge direction, respectively. Inset: FFT of panel (b). The diffraction spots corresponding to the graphene lattice are marked by white circles (scanning conditions for the images: (a) −300 mV, 0.9 nA; inset: −150 mV, 1.2 nA; (b) −15 mV, 2 nA).

Figure 4 shows a different type of edge. The top layer displays a moiré pattern with a period of about 4.9 nm and the bottom one does not. This means that there is no rotation between the bottom layer and the third layer. The atomic lattices in both layers are simultaneously resolved in Fig. 4(b). This gives the rotation between the two layers of about 2.8°. Consequently in the FFT obtained from Fig. 3(b), there are two sets of spots in the white circles rotated by 2.8°. These directly measured values of 2.8° and 4.9 nm validate equation 1, as illustrated by the simulation shown in Fig. 4(d). On the bottom layer without moiré, again only one sublattice is observable, while on the layer with moiré, both sublattices are seen. This edge is along the zigzag direction of the top layer. The smaller hexagonal pattern in the FFT corresponds to the scattering pattern in Fig. 4(b), which is quite close to $(\sqrt{3}\times\sqrt{3})R30°$. In

studies of monolayer edges, a honeycomb scattering pattern has only been observed around the armchair edges. However, a honeycomb scattering pattern is also seen here close to the zigzag edge. Again, we note that this edge is not a monolayer zigzag edge because of the existence of the layers underneath.

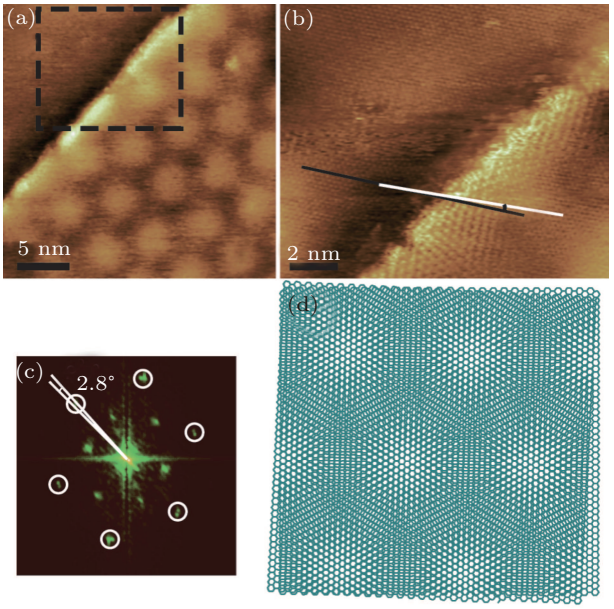


Fig. 4. (color online) STM results at another step edge. (a) There are (not) moiré patterns in the top (bottom) layer. (b) Atomically resolved image of the boxed area in panel (a), showing a rotation angle of 2.8°and a scattering pattern. The edge is along the zigzag direction of the top layer. (c) FFT of panel (b) showing two sets of diffraction spots of the graphene lattices (marked by white circles) and one set of the scattering pattern. (d) Simulation of the moiré pattern with a 2.8° rotation (scanning conditions for the images: (a) −300 mV, 0.5 nA; (b) −15 mV, 1.2 nA).

The moiré patterns observed in our samples have many different periods, some of which are listed in Table 1. The typical corrugation of the moiré superstructures is 0.2–0.5 Å, which is similar to those observed on Ir(111)[37] and much smaller than that on Ru(0001).[38] Most of the moiré patterns are commensurate with the twist angle satisfying $\cos\theta = (6i^2+6i+1)/(6i^2+6i+2)$, where i is any positive integer. Figure 5 shows moiré patterns with periods of 3.6 nm and 6.2 nm. When trying to get atomic resolution with bias smaller than 200 mV, we found that in regions without moiré only one sublattice was apparent. This can be explained because in AB stacking the sublattice right atop the carbon atoms of the second layer has a much lower local density of states than the other, resulting in dark carbon sites in STM images.[30] On the other hand, both sublattices were always seen in regions with moiré patterns. This phenomenon was mentioned above in Figs. 3 and 4. Two more examples are shown in Fig. 5. This can be understood as a consequence of the rotation, there are no sublattices right atop the carbon atoms of the second layer, the two sublattices largely return to equivalence. In other words, interlayer rotation can determine the observation of both or one sublattice.

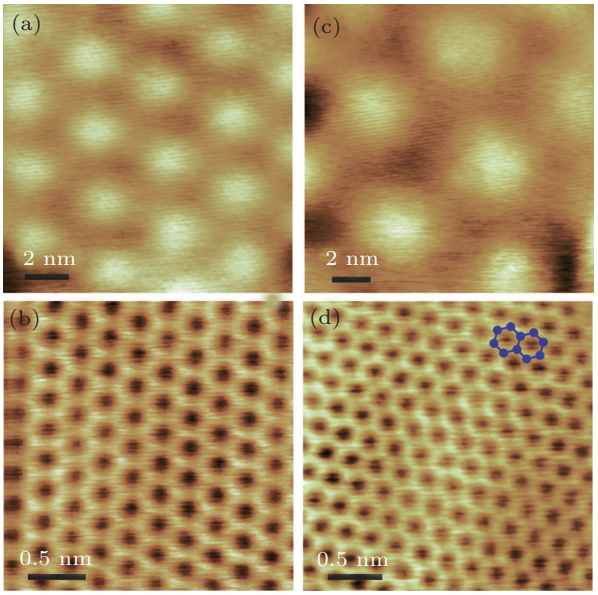


Fig. 5. (color online) STM images of moiré patterns with periods of 3.6 nm (a) and 6.2 nm (c). (b) and (d) Atomically resolved STM images obtained in regions in panels (a) and (c), respectively, showing both sublattices (scanning conditions for the images: (a) −60 mV, 2.0 nA; (b) −15 mV, 2.0 nA; (c) −200 mV, 1.0 nA; (d) −20 mV, 2.0 nA).

Table 1. Some moiré pattern periods observed in this study.

Period/nm	2.76	3.2	3.6	4.9	6.2	7.1
Rotation/(°)	5.1	4.4	3.9	2.8	2.3	2.0

4. Conclusion

In summary, few-layer graphene grown on Ni thin films has been characterized by STM. Moiré patterns dominate on these samples. They originate from the rotations between two consecutive layers. At low bias, only one sublattice shows up in STM in regions without moiré (AB stacking), while both sublattices are seen in regions with moiré (rotation). Step edges are abundant on the topmost graphene layers, showing various orientations with respect to the two layers involved. The scattering characteristics vary accordingly, which are different from those at armchair or zigzag monolayer graphene edges. This FLG/Ni system exhibits a wealth of rotational stacking and edge configurations, thus providing a nice template for studying related properties.

References

[1] Mak K F, Lui C H, Shan J and Heinz T F 2009 *Phys. Rev. Lett.* **102** 256405
[2] Kim K S, Walter A L, Moreschini L, Seyller T, Horn K, Rotenberg E and Bostwick A 2013 *Nat. Mater.* **12** 887
[3] Li G H, Luican A, dos Santos J M B L, Neto A H C, Reina A, Kong J and Andrei E Y 2010 *Nat. Phys.* **6** 109
[4] Lui C H, Li Z Q, Chen Z Y, Klimov P V, Brus L E and Heinz T F 2011 *Nano Lett.* **11** 164
[5] He R, Chung T F, Delaney C, Keiser C, Jauregui L A, Shand P M, Chancey C C, Wang Y N, Bao J M and Chen Y P 2013 *Nano Lett.* **13** 3594
[6] Singh M K, Titus E, Goncalves G, Marques P, Bdikin I, Kholkin A L and Gracio J J A 2010 *Nanoscale* **2** 700

[7] Mak K F, Shan J and Heinz T F 2010 *Phys. Rev. Lett.* **104** 176404
[8] Hao X, Chen Y F, Li P J, Wang Z G, Liu J B, He J R, Fan R, Sun J R, Zhang W L and Li Y R 2012 *Chin. Phys. B* **21** 046801
[9] Pan Y, Shi D X and Gao H J 2007 *Chin. Phys.* **16** 3151
[10] Bistritzer R and MacDonald A H 2011 *PNAS* **108** 12233
[11] Reina A, Jia X T, Ho J, Nezich D, Son H B, Bulovic V, Dresselhaus M S and Kong J 2009 *Nano Lett.* **9** 30
[12] Li X S, Cai W W, An J H, Kim S, Nah J, Yang D X, Piner R, Velamakanni A, Jung I, Tutuc E, Banerjee S K, Colombo L and Ruoff R S 2009 *Science* **324** 1312
[13] Mun J H, Hwang C, Lim S K and Cho B J 2010 *Carbon* **48** 447
[14] Thiele S, Reina A, Healey P, Kedzierski J, Wyatt P, Hsu P L, Keast C, Schaefer J and Kong J 2010 *Nanotechnology* **21** 015601
[15] Cao H L, Yu Q K, Colby R, Pandey D, Park C S, Lian J, Zemlyanov D, Childres I, Drachev V, Stach E A, Hussain M, Li H, Pei S S and Chen Y P 2010 *J. Appl. Phys.* **107** 044310
[16] Obraztsov A N, Obraztsova E A, Tyurnina A V and Zolotukhin A A 2007 *Carbon* **45** 2017
[17] Gao M, Pan Y, Zhang C D, Hu H, Yang R, Lu H L, Cai J M, Du S X, Liu F and Gao H J 2010 *Appl. Phys. Lett.* **96** 053109
[18] Varchon F, Mallet P, Magaud L and Veuillen J Y 2008 *Phys. Rev. B* **77** 165415
[19] Wang M and Li C M 2011 *Nanoscale* **3** 2324
[20] Nakada K, Fujita M, Dresselhaus G and Dresselhaus M S 1996 *Phys. Rev. B* **54** 17954
[21] Orlof A, Ruseckas J and Zozoulenko I V 2013 *Phys. Rev. B* **88** 125409
[22] Ouyang F P, Chen L J, Xiao J and Zhang H 2011 *Chin. Phys. Lett.* **28** 047304
[23] Rutter G M, Crain J N, Guisinger N P, Li T, First P N and Stroscio J A 2007 *Science* **317** 219
[24] Yang H, Mayne A J, Boucherit M, Comtet G, Dujardin G and Kuk Y 2010 *Nano Lett.* **10** 943
[25] Tian J F, Cao H L, Wu W, Yu Q K and Chen Y P 2011 *Nano Lett.* **11** 3663
[26] Enoki T, Fujii S and Takai K 2012 *Carbon* **50** 3141
[27] Brihuega I, Mallet P, Gonzalez-Herrero H, de Laissardiere G T, Ugeda M M, Magaud L, Gomez-Rodriguez J M, Yndurain F and Veuillen J Y 2012 *Phys. Rev. Lett.* **109** 196802
[28] Kuwabara M, Clarke D R and Smith D A 1990 *Appl. Phys. Lett.* **56** 2396
[29] Binnig G, Fuchs H, Gerber C, Rohrer H, Stoll E and Tosatti E 1986 *Europhys. Lett.* **1** 31
[30] Tomanek D, Louie S G, Mamin H J, Abraham D W, Thomson R E, Ganz E and Clarke J 1987 *Phys. Rev. B* **35** 7790
[31] Ouseph P J, Poothackanal T and Mathew G 1995 *Phys. Lett. A* **205** 65
[32] Wang Y F, Ye Y C and Wu K 2006 *Surf. Sci.* **600** 729
[33] Liu N, Fu L, Dai B Y, Yan K, Liu X, Zhao R Q, Zhang Y F and Liu Z F 2011 *Nano Lett.* **11** 297
[34] Lahiri J, Lin Y, Bozkurt P, Oleynik II and Batzill M 2010 *Nat. Nanotechnol.* **5** 326
[35] Chae S J, Gunes F, Kim K K, Kim E S, Han G H, Kim S M, Shin H J, Yoon S M, Choi J Y, Park M H, Yang C W, Pribat D and Lee Y H 2009 *Adv. Mater.* **21** 2328
[36] Zhang X Y, Xin J and Ding F 2013 *Nanoscale* **5** 2556
[37] Coraux J, N'Diaye A T, Busse C and Michely T 2008 *Nano Lett.* **8** 565
[38] Marchini S, Günther S and Wintterlin J 2007 *Phys. Rev. B* **76** 075429